Synthesis and Mass Spectrometry Studies of Branched Oxime Ether Libraries. Mapping the Substitution Motif via Linker Stability and Fragmentation Pattern

Noureddin Nazarpack-Kandlousy,[†] Marina I. Nelen,[†] Vasiliy Goral,[†] and Alexey V. Eliseev*[,†,‡]

Department of Chemistry, State University of New York at Buffalo, Buffalo, New York 14260, and Therascope AG, Hans-Bunte-Str. 20, 69123 Heidelberg, Germany

eliseev@buffalo.edu

Received May 17, 2001

The oxime ether chemistry has recently been used as a convenient approach to preparing potentially highly diverse combinatorial libraries. The synthetically easiest way to form the libraries is convergent, i.e., via reaction of a branched scaffold containing two or more aminooxy linker groups, with a variety of carbonyl substituents. We show here that such reactions between aldehydes and ketones of different structure with the scaffolds containing different types of aminooxy groups can lead to the formation of virtually all expected components in the model mixtures **1**−**3** formed from three scaffolds (**7**−**9**) and eight substituents (R_1−R_8). One important problem with the branched libraries is that the libraries formed from the more complex scaffolds, such as **11**, contain multiple regioisomers. The results of extensive analysis of a variety of library components by mass spectrometry presented here show that the differences in the MS−MS fragmentation energies for different linkers yield regiochemical information essential for identification of individual library components.

Introduction

Combinatorial chemistry and related techniques of organic synthesis have been rapidly developing over the recent years as tools for efficient generation of large arrays of compounds for biological screening.[1−7] It is now clear that, even with the most efficient combinatorial synthesis methods, it is not possible to cover the full desired diversity space even for small drug-like molecules. Still, there is a big demand for new synthetic and analytical approaches that can quickly generate and assess large number of diverse chemical structures. Most of the organic compound libraries, e.g., in the pharmaceutical industry, are synthesized by parallel techniques as arrays of individual compounds. A potentially much faster approach to molecular diversity is the formation of mixture libraries[8−11] via a convergent or divergent combination of building blocks. The mixture formation is attractive in its simplicity, but to fit in an overall high-throughput synthesis/screening strategy, it has to be complemented by appropriate methods for screening and structure identification of individual components.

The oxime ether chemistry and the relevant chemistry of aminooxy compounds[12−15] has recently attracted attention as a convenient approach to the rapid formation of combinatorial libraries, both in a divergent[16,17] and in a convergent[18] mode. In the divergent case, the libraries are formed by the reaction of a scaffold containing two or more aminooxy groups with a mixture of carbonyl compounds (Scheme 1). The reaction proceeds under mild conditions and is rapid and selective in that the carbonyl groups are preferred over the majority of other functionalities capable of reacting with the aminooxy nucleophile. The resulting libraries have been shown to contain an excellent representation of the expected components that are formed from aldehydes with varying steric and electronic properties.[16] Among other advantages of the oxime ethers is their potential suitability[19] as components for the dynamic libraries.[20−24]

[†] State University of New York at Buffalo.
[‡] Therascope AG.

(1) Lowe, G. *Chem. Soc. Rev.* **1995**, *24*, 309 ff.
(2) Thompson, L. A.; Ellman, J. A. *Chem. Rev.* **1996**, *96*, 555−600.
(3) Balkenhohl, F.; Von dem Bussche-Hunnenfeld, C.; Lansky, A.; Zechel, C. *Angew. Chem., Int. Ed. Engl.* **1996**, *35*, 2289−2337.
(4) Patel, D. V.; Gordon, E. M. *Drug Discov. Today* **1996**, *1*, 134−144.
(5) Williard, X.; Pop, I.; Bourel, L.; Horvath, D.; Baudelle, R.; Melnyk, P.; Deprez, B.; Tartar, A. *Eur. J. Med. Chem.* **1996**, *31*, 87−98.
(6) Maehr, H. *Bioorg. Med. Chem.* **1997**, *5*, 473−491.
(7) Weber, L. *Curr. Opin. Chem. Biol.* **2000**, *4*, 295−302.
(8) Blondelle, S. E.; Crooks, E.; Ostresh, J. M.; Houghten, R. A. *Antimicrob. Agents Chemother.* **1999**, *43*, 106−114.
(9) Houghten, R. A.; Pinilla, C.; Appel, J. R.; Blondelle, S. E.; Dooley, C. T.; Eichler, J.; Nefzi, A.; Ostresh, J. M. *J. Med. Chem.* **1999**, *42*, 3743−3778.
(10) Houghten, R. A.; Wilson, D. B.; Pinilla, C. *Drug Discov. Today* **2000**, *5*, 276−285.
(11) Teixido, J.; Michelotti, E. L.; Tice, C. M. *J. Comb. Chem* **2000**, *2*, 658−674.
(12) Khomutov, A. R.; Vepsalainen, J. J.; Shvetsov, A. S.; Hyvonen, T.; Keinanen, T. A.; Pustobaev, V. N.; Eloranta, T. O.; Khomutov, R. M. *Tetrahedron* **1996**, *52*, 13751−13766.
(13) Choong, I. C.; Ellman, J. A. *J. Org. Chem.* **1999**, *64*, 6528−6529.
(14) Kuksa, V.; Buchan, R.; Lin, P. K. T. *Synthesis* **2000**, 1189−1207.
(15) Petrassi, H. M.; Sharpless, K. B.; Kelly, J. W. *Org. Lett* **2001**, *3*, 139−142.
(16) Nazarpack-Kandlousy, N.; Zweigenbaum, J.; Henion, J.; Eliseev, A. V. *J. Comb. Chem.* **1999**, *1*, 199−206.
(17) Nazarpack-Kandlousy, N.; Chernushevich, I. V.; Meng, L. J.; Yang, Y.; Eliseev, A. V. *J. Am. Chem. Soc.* **2000**, *122*, 3358−3366.
(18) Maly, D. J.; Choong, I. C.; Ellman, J. A. *Proc. Natl. Acad. Sci. U.S.A.* **2000**, *97*, 2419−2424.
(19) Polyakov, V. A.; Nelen, M. I.; Nazarpack-Kandlousy, N.; Ryabov, A. D.; Eliseev, A. V. *J. Phys. Org. Chem.* **1999**, *12*, 357−363.
(20) Ganesan, A. *Angew. Chem., Int. Ed. Engl.* **1998**, *37*, 2828−2831.
(21) Eliseev, A. V.; Lehn, J. M. *Comb. Chem. Biol.* **1999**, *243*, 159−172.

10.1021/jo015765j CCC: $22.00
Published on Web 12/07/2001

Scheme 1

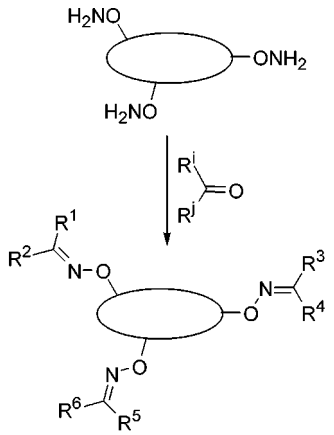

One of the inherent problems with the structures shown in Scheme 1, and with the branched libraries overall, is the simultaneous formation of multiple regioisomers, which are difficult to characterize structurally, particularly when in a mixture with similar compounds. We have addressed this problem previously via a combined synthetic/analytical approach (regiochemical tagging)[17] that involved synthesis of isotopically labeled aminooxy scaffolds. In the ensuing paper, we show that the intrinsic gas-phase properties of the oxime ether library components make it possible to assign their structure via straightforward analysis using tandem mass spectrometry, and in many cases without invoking special tagging procedures. It is also shown that the synthesis and analysis of the oxime ether libraries can incorporate a broad range of building blocks, such as variety of aromatic and aliphatic aldehydes and ketones, with different steric and electronic properties.

Results and Discussion

We have previously shown that the stability of oxime ether linker groups in the collision-induced dissociation MS−MS analysis is sensitive to the chemical environment of the linker.[17] This fact played a useful role in the structural identification of the components, because substituents linked to different attachment points were cleaved off at different energies, and the regiochemistry of the compound could thus be determined.

To explore the chemistry of the oxime ethers in a combinatorial context, it was important to test diverse types of both scaffolds and substituents in the formation of library components, as well as to assess their suitability for structural analysis by mass spectrometry. Initially, we synthesized three types of libraries **1**−**3** on the basis of disubstituted scaffolds **7**−**9**, respectively, each with two identical aminoxy groups. The synthetic routes for the aminooxy scaffolds are depicted in Scheme 2. To compare the properties of different substituents, we tested different types of aldehydes and ketones, both aliphatic and aromatic (R_1−R_8), with all three scaffolds.

The compounds for mass-spectrometry studies were prepared in the form of small mixture libraries resulting from the condensations of the scaffolds with two to four carbonyl substituents. The condensation products included all of the expected components, even those resulting from carbonyls with different electronic and steric properties. While the exact ratio of products could not be precisely determined by mass spectrometry, due to the lack of individual standard compounds, all predicted oxime ether components appeared as molecular peaks in the single MS spectra (Figure 1). This fact simplified the subsequent structural studies and supported previously made conclusion about low selectivity of the oximation reaction.[16,17]

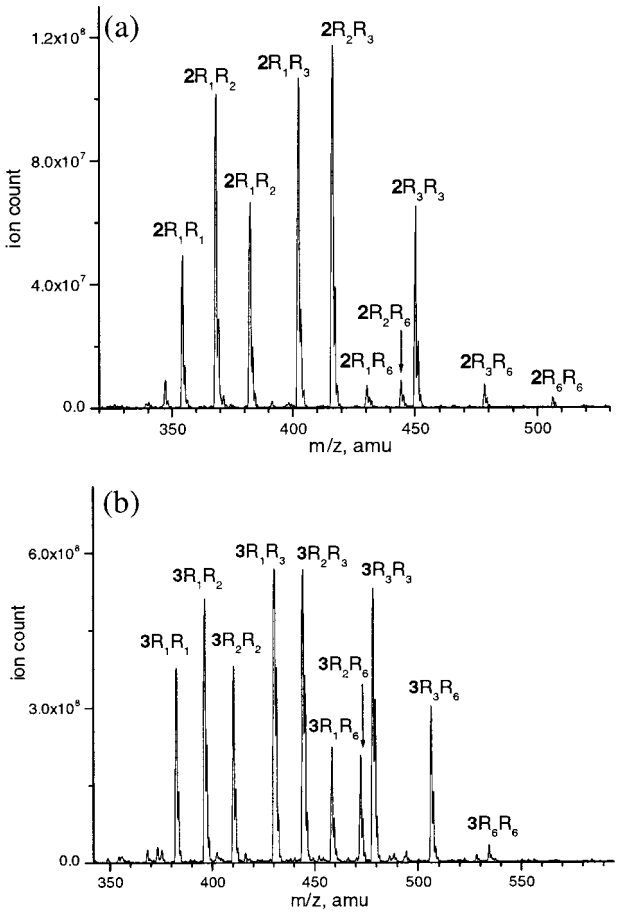

Figure 1. ESI MS of the mixture libraries **2** (a) and **3** (b) formed by mixing scaffolds **8** and **9**, respectively, with four carbonyl compounds R_1=O, R_2=O, R_3=O, R_6=O.

The molecular peaks of the oxime ether library components in the single MS were then subjected to collision-induced dissociation[25] in a triple quadrupole mass spectrometer. We were particularly interested in observing the "informative" fragments that correspond to the cleavage of substituents from the scaffolds, allowing the identification of the substitution motif. The collision energies were optimized for maximum intensity of each fragment, and the optimal values were used to characterize the stability of the fragmented bonds in the gas phase. The three sets of disubstituted compounds (**1**−**3**) showed differences both in the fragmentation energies and the fragment patterns, as summarized in Table 1.

Among the major fragments from libraries **1** and **2** were those resulting from the homolytic cleavage of the N−O bonds. One of the reasons for testing these libraries was to reinforce our earlier finding that the presence of

(22) Lehn, J. M. *Chem. Eur. J.* **1999**, *5*, 2455−2463.
(23) Cousins, G. R. L.; Poulsen, S. A.; Sanders, J. K. M. *Curr. Opin. Chem. Biol.* **2000**, *4*, 270−279.
(24) Lehn, J. M.; Eliseev, A. V. *Science* **2001**, *291*, 2331−2332.
(25) Busch, K. L.; Glish, G. L.; McLuckey, S. A. *Mass Spectrometry/Mass Spectrometry*; VCH Publishers: Weinheim, Germany, 1988.

Scheme 2[a]

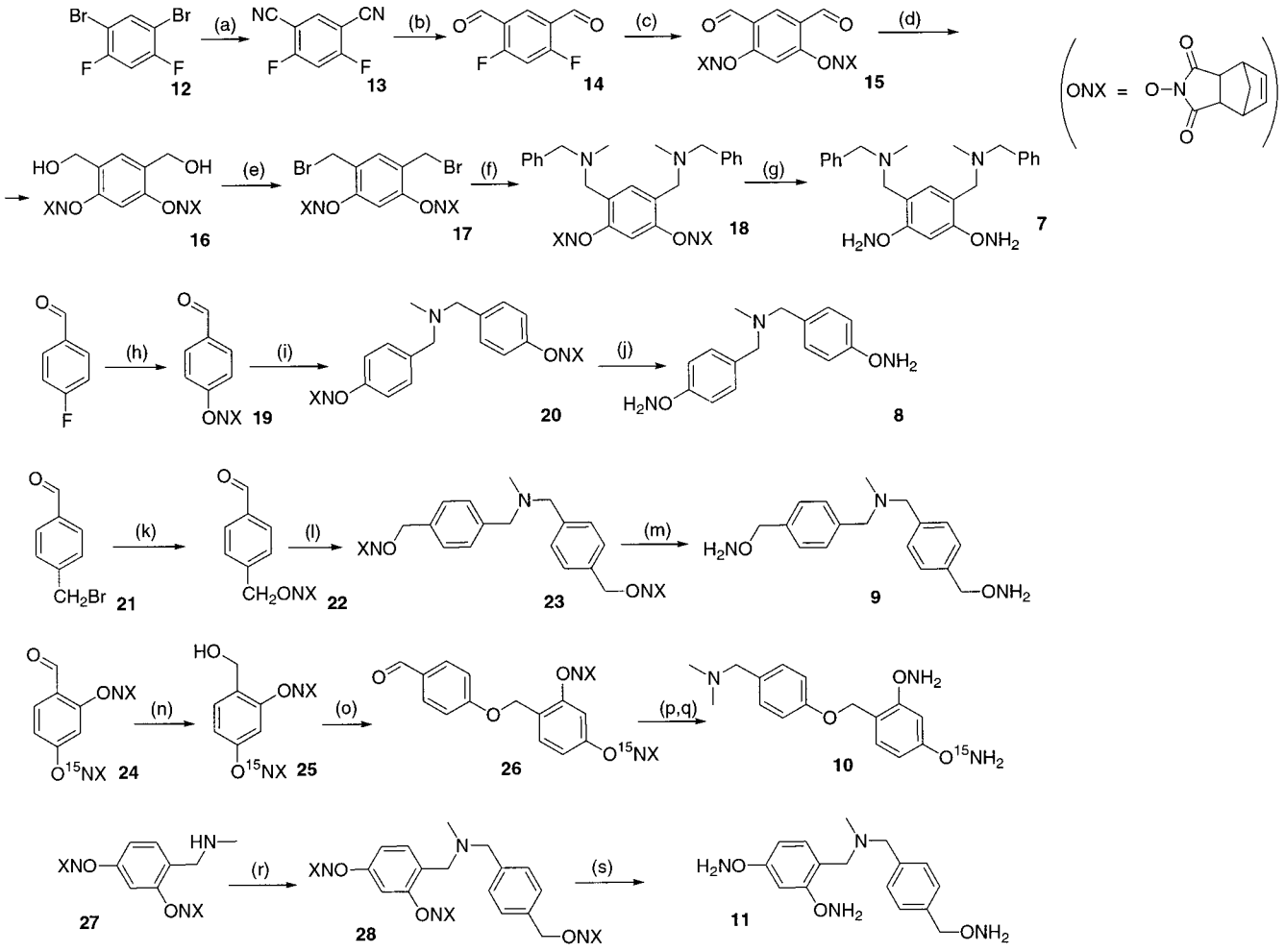

[a] Legend: (a) CuCN, DMF, 150 °C, 17 h, 37%; (b) DIBAL-H, toluene, 0 °C, 1 h, 67%; (c) HONX/K_2CO_3, DMF, rt, 1 h, 97%; (d) $NaBH_3CN$/Ti(O-*i*-Pr)$_4$, $CHCl_3$/MeOH, rt, 1 h, 45%; (e) PBr_3, CH_2Cl_2/ether, rt, 3 h, 75%; (f) MeBnNH/K_2CO_3, DMSO, rt, 2 h, 95%; (g) N_2H_4·H_2O, CD_3OH/$CDCl_3$, rt, 12 h, 50%; (h) HONX/K_2CO_3, DMF, 75 °C, 3 h, 56%; (i) $MeNH_2$/$NaBH_3CN$/Ti(O-*i*-Pr)$_4$, $CHCl_3$/MeOH, rt, 1 h, 45%; (j) N_2H_4·H_2O, CD_3OH/$CDCl_3$, rt, 2 h, 55%; (k) HONX/K_2CO_3, DMSO, rt, 1 h, 96%; (l) $MeNH_2$/$NaBH_3CN$/Ti(O-*i*-Pr)$_4$, $CHCl_3$/MeOH, rt, 1 h, 50%; (m) N_2H_4·H_2O, CD_3OH/$CDCl_3$, rt, 3 h, 60%; (n) $NaBH_3CN$/Ti(O-*i*-Pr)$_4$, $CHCl_3$/MeOH, rt, 1 h, 64%; (o) CH_2Cl_2, PPh_3, DEAD, rt, 10 h, 82%; (p) $MeNH_2$.HCl, $NaBH_3CN$/Ti(O-*i*-Pr)$_4$, $CHCl_3$/MeOH, rt, 1 h, 52%; (q) N_2H_4·H_2O, CD_3OH/$CDCl_3$, rt, 15 h, 50%; (r) **22**, Ti (O-*i*-Pr)$_4$, $NaBH_3CN$, $CHCl_3$/MeOH, 50%;(s) N_2H_4·H_2O, CD_3OH/$CDCl_3$, rt, 2.5 h, 60%.

substituents in the position ortho to the O−N=R group facilitates the fragment formation. Indeed, the results showed that the cleavage of substituents from **1** was typically observed in the energy range between 10 and 17 eV, while similar cleavage in **2** required 17−20 eV. Similar positional effects had been observed previously in the compounds with both ortho and para substituents;[17] however, only here were we able to quantify the energy difference. Based on our studies of libraries **4**, we proposed previously that the low energy of the ortho substituent cleavage might be due to assistance of the neighboring protonated amino group. In the current study, we tested this hypothesis with library **5** formed from scaffold **10** in which the protonated amino group was separated from the fragmentation center by a rigid substituent. The MS−MS spectra of **5** showed a difference between the ortho and para substituent cleavage energies similar to **4**, which indicates that difference is most likely due to steric effects. (MS−MS of **4** and **5** was performed on a QqTOF mass spectrometer (Sciex), while the spectra of other libraries were recorded on the triple quadrupole instrument. Therefore, the fragmentation energies could not be directly compared between these series of compounds.)

The MS−MS of libraries **3** showed a somewhat different fragmentation pattern. The presence of hydrogen in the beta-position to the oxime nitrogen led to the loss of the substituent fragment of one mass unit higher, apparently resulting from the hydrogen abstraction from the CH_2 group (Scheme 3). However, the optimum energy needed for cleaving the substituent increased dramatically, to 30−35 eV. This observation points to the much higher stability of the aliphatic O−N=R group, as compared to aromatic.

Nearly all of the fragments observed at less than 35 eV contained some part of the central scaffold. This fact is not surprising because the electrospray ionization is known to preserve the solution chemistry of the ions,[26] where the ionic charge is concentrated on the nitrogen of the amino groups. However, for structural analysis it is particularly attractive to be able to directly observe fragments of the substituents, which became possible in

(26) Hofstadler, S. A.; Bakhtiar, R.; Smith, R. D. *J. Chem. Educ.* **1996**, *73*, A 82 ff.

Chart 1

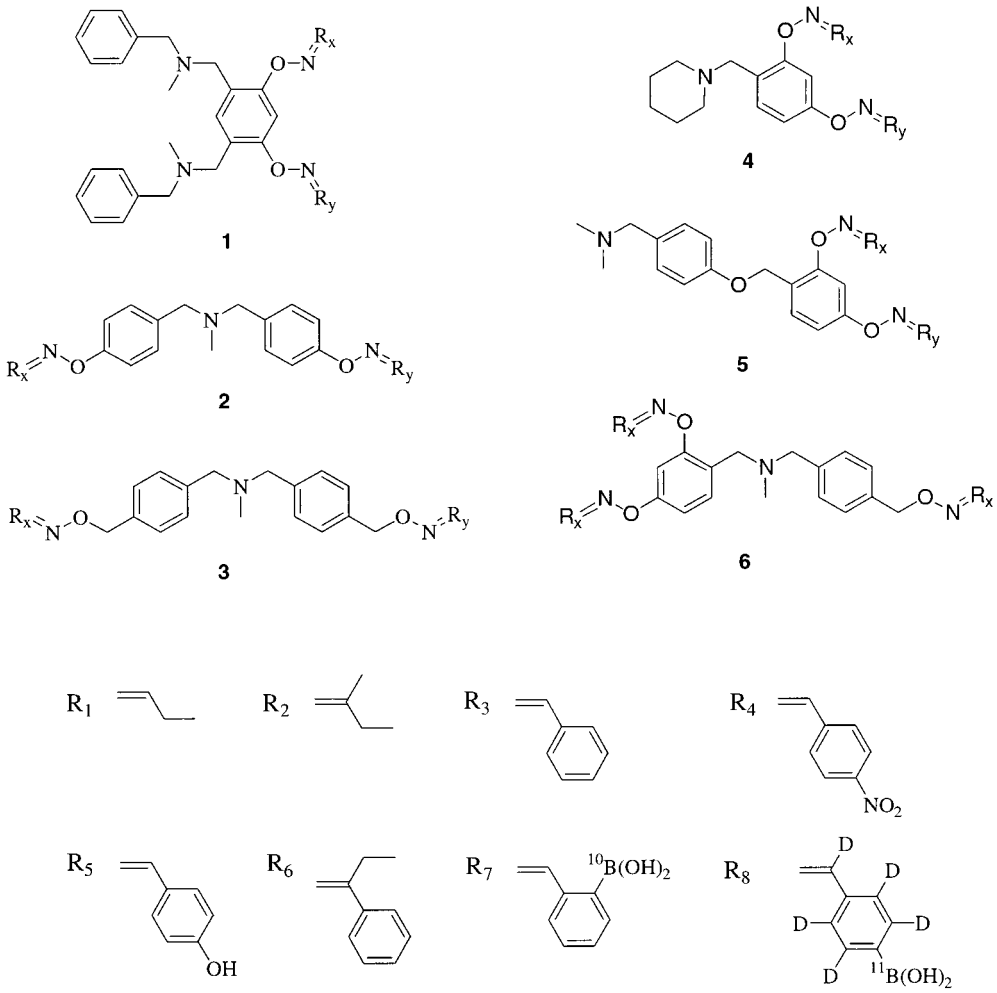

the case of aliphatic oxime ethers **3**. At the fragmentation energies above 40 eV, peaks of the RN^+ type were detected in the positive ionization mode MS−MS for a variety of substituents (Table 1). The relative intensity of the peaks was dependent on the electronic properties of the aldehyde and varied from barely visible (R_4) to the most intense in the spectrum (R_5). However, the corresponding peaks from all substituents could always be detected, even in the compound containing both R_4 and R_5. These types of fragments were never observed in the aromatic oxime ethers **1** and **2**, nor in the previously studied scaffolds.[17] We believe that these fragments result from direct heterolytic cleavage, as shown in Scheme 3. The scaffold part of the cleavage (M + H − RN) was not observed in the spectrum, being neutral overall.

The experiments with the disubstituted scaffolds demonstrate (i) that different types of the oxime ether linkages exhibit different fragmentation energies and patterns and (ii) that these differences are by and large determined by the variation of the scaffold structure, and to a much lesser degree by the types of substituents. Therefore, by combining different types of linkages in more complex scaffolds, one should be able to determine the regiochemistry of a variety of library components, i.e., to obtain the fragment of each substituent with a unique energy and pattern, which is characteristic of its attachment position. This hypothesis was tested with libraries **6** based on trisubstituted scaffold **11**.

The reaction of **11** with more than one carbonyl compound leads to the formation of multiple isomers that show up as one peak and make the MS−MS energy analysis difficult. Hence, we restricted the MS studies to the corresponding oxime ethers with three identical substituents (Table 2). These individual compounds bore the combination of linkers of the three previously studied types, i.e., ortho- and para-substituted aromatic and aliphatic oxime ethers. Even though the fragmentation of **6** was expected to cleave off chemically similar substituents, the difference in the linkers would result in different energy optima and the fragment pattern.

The fragments resulting from the first substituent cleavage (MH − R_xN) had optimum energies in the range somewhat higher than that observed for **1**. Because in this case we could not distinguish between the fragments with the remaining ortho and para substituents, the optimization graph shown in Figure 2 most likely reflects the combination of both fragments and results in the average energy. However, as shown above with disubstituted scaffolds, similar fragmentation performed on the compound with different substituents should show a distinct difference in the energy optima and clearly identify the position of each of the substituents. Unlike libraries **1**−**3**, structures **6** generated a new type of informative fragments, MH − $(RxN)_2$, with the optimum energy between 25 and 32 eV. In the disubstituted **1**−**5**, similar fragments were always observed, but represented the bare central moiety and therefore did not provide any

Table 1. Optimal Fragmentation Energies for the Series of Compounds 1−3

scaffold	substituents (R_x,R_y)	characteristic fragments (positive mode)	maxima of fragment intensity vs collision energy plots, ±0.5 eV
1	R_1, R_1	MH−R_1N	12.5
1	R_1, R_2	MH−R_1N	11.0
		MH−R_2N	13.0
1	R_1, R_3	MH−R_1N	11.5
		MH−R_3N	13.5
1	R_1, R_6	MH−R_1N	10.1
		MH−R_6N	15.2
1	R_3, R_4	MH−R_3N	16.0
		MH−R_4N	12.5
1	R_3, R_5	MH−R_3N	11.7
		MH−R_5N	13.4
1	R_3, R_6	MH−R_3N	11.5
		MH−R_6N	15.4
1	R_4, R_5	MH−R_4N	12.0
		MH−R_5N	17.0
1	R_7, R_7	MH−R_7N	13.2
1	R_7, R_8	MH−R_7N	13.3
		MH−R_8N	13.0
1	R_8, R_8	MH−R_8N	13.0
2	R_1, R_1	MH−R_1N	16.8
2	R_1, R_2	MH−R_1N	16.7
		MH−R_2N	17.0
2	R_1, R_3	MH−R_1N	17.0
		MH−R_3N	17.5
2	R_2, R_2	MH−R_2N	17.3
2	R_2, R_3	MH−R_2N	17.0
		MH−R_3N	17.0
2	R_3, R_3	MH−R_3N	17.8
2	R_3, R_4	MH−R_3N	20.0
		MH−R_4N	17.0
2	R_3, R_5	MH−R_3N	17.5
		MH−R_5N	18.0
2	R_4, R_4	MH−R_4N	20.0
2	R_5, R_5	MH−R_5N	17.5
3	R_1, R_1	MH−R_1NH	29.0
3	R_3, R_3	MH−R_3NH	32.0
		R_3N	37.5
3	R_3, R_4	MH−R_3NH	35.0
		R_3N	47.0
		R_4N	54.0
3	R_3, R_5	MH−R_3NH	35.0
		MH−R_5NH	29.0
		R_3N	40.5
		R_5N	43.0
3	R_4, R_4	MH−R_4NH	37.5
		R_4N	54.0
3	R_4, R_5	MH−R_5NH	35.0
		R_4N	27.5
		R_5N	40.0
3	R_5, R_5	MH−R_5NH	35.0
		R_5N	50.0

regiochemical information. In contrast, this type of fragmentation in **6** is important because it shows what substituent remains on the more stable aliphatic linker. The latter piece of information can be confirmed by detecting the RxN fragments coming off at yet higher energy from the aliphatic linker (Table 2).

Although the above studies of **6** have been performed with individual compounds, they have clear implications for the analysis of libraries based on **11** or similar scaffolds. The observation of the substituent cleavage at different energies from different positions bears important regiochemical information about the parent compounds. Thus, if an individual library component based on type **6** or similar scaffolds were isolated, e.g., after affinity selection with a biological target, then its substitution motif could be mapped by the MS−MS analysis at varying energies. The new fragmentation patterns discovered in the aliphatic oxime ethers allow one to proofread the structural identification based on different types of fragments.

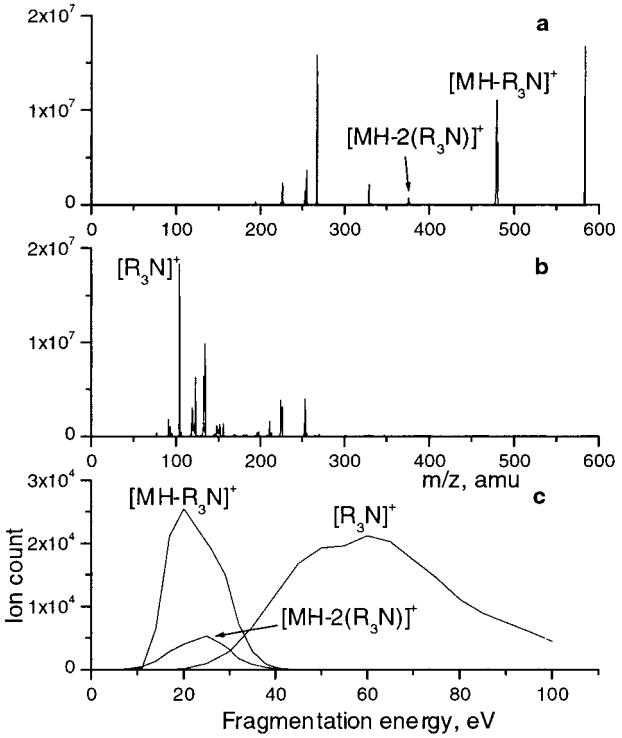

Figure 2. ESI MS−MS of the parent peak of compound **6**$(R_3)_3$ at 13 eV (a) and 50 eV (b) and energy optimization curves (c) for different fragments.

Scheme 3

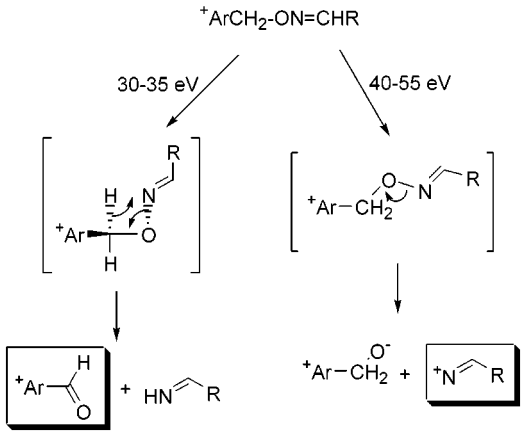

Table 2. Characteristic Fragment Energies for the Series of Compounds 6

R_x	fragment	optimum of collision energy, ±0.5 eV
R_1	MH−R_1N	15.0
	MH−$(R_1N)_2$	25.0
	R_1N	65.5
R_2	MH−R_2N	11.5
	MH−$(R_2N)_2$	29.0
	R_2N	48.0
R_3	MH−R_3N	20.0
	MH−$(R_3N)_2$	25.0
	R_3N	55.0
R_6	MH−R_6N	20.0
	MH−$(R_6N)_2$	31.5
	R_6N	40.0

Conclusion

This study has shown that minor structural variations in the oxime ether linkers utilized with branched polysubstituted structures can allow one to determine the

regiochemistry of substitution by mass spectrometry. In combination with the previously developed regiochemical tagging method,[17] this approach leverages the practical application of mixture-based combinatorial libraries, and specifically those with labile linkers such as oxime ethers. It is theoretically possible to synthesize complex branched scaffolds or even dendrimers with a variety of attachment points and rapidly generate vast diversity of compounds in one pot (specific oxime ether chemistry is particularly advantageous, because it gives access to the large array of commercially available aldehydes and ketones). The attachment points in the scaffolds can be differentiated either by fragmentation energies and patterns, or with the isotopic labeling motif. The MS−MS properties of the scaffolds can be studied with a few symmetrically substituted compounds and then the trends identified can potentially be applied to the structural analysis of complex library components.

Experimental Section

Mass spectrometry analysis was performed using a model API-3000 triple quadrupole mass spectrometer (Applied Biosystem/Sciex, USA) coupled to LC and equipped with a turbo ionspray interface. The mass spectrometer was operated at a unit resolution. Samples were introduced into the ionization source at a flow rate of 5 μL/min with a syringe pump. The ionspray needle was operated at +5500 V, and the orifice voltage was set at 35−40 eV. Full-scan MS spectra were acquired over the mass range m/z 50−1000 by scanning the first quadrupole (Q1) with 0.1 step size at a scan rate of 2 s. The product-ion spectra were obtained with collision energy ranging from 5 to 60 eV.

The optimum of collision energy for each certain fragmentation was determined as collision energy corresponding to the maximum of a characteristic fragment-ion peak. The optimization was performed with collision energy varying from 5 to 100 eV at a step size of 3−5 eV.

Solutions were prepared in 25% (v/v) aqueous acetonitrile with sample concentration ranging from 5 to 30 μM.

Synthesis. 1,5-Dibromo-2,4-difluorobenzene (12) was synthesized on the basis of the procedure used for the synthesis of 5-bromo-2,4-difluorotoluene.[27] The pure product was obtained in 75% yield after distillation (35−38 °C, 2 mmHg). ^{1}H NMR (δ ppm, 500 MHz, $CDCl_3$): 7.76 (t, J = 7.3 Hz, 1H), 7.00 (t, J = 8.3 Hz, 1H). ^{13}C NMR (δ ppm, 125 MHz, $CDCl_3$): 158.36 (dd, J_1 = 11.3 Hz, J_2 = 250 Hz), 136.33 (t, J = 1.1 Hz), 105.78 (t, J = 26.9 Hz), 104.55 (dd, J_1 = 8.9 Hz, J_2 = 17.4 Hz). FAB MS: 269.8, 271.8, 273.8 ([M + H]$^+$, Br isotopes).

4,6-Difluoroisophthalonitrile (13). To 8.16 g (30 mmol) of **12** in 100 mL of DMF was added 6.18 g (69 mmol) of cuprous cyanide. The mixture was refluxed for 17 h and then cooled to room temperature. After the mixture was passed through a filter and solvent evaporated, it was stirred in a mixture of 200 mL of CH_2Cl_2 and 50 mL of ice-cold water. The mixture was extracted with additional 2 × 50 mL of CH_2Cl_2, and the combined organic layers were washed with 3 × 100 mL of water, filtered, and dried over anhydrous $MgSO_4$. The solvent was then evaporated, and the crude mixture was purified by silica chromatography (10−40% of hexanes in CH_2Cl_2) to yield 1.82 g (37%) of **13**. ^{1}H NMR (δ ppm, 500 MHz, $CDCl_3$): 8.04 (t, J = 6.8 Hz, 1H), 7.24 (t, J = 8.5 Hz, 1H). ^{13}C NMR (δ ppm, 125 MHz, $CDCl_3$): 166.04 (dd, J_1 = 13.5 Hz, J_2 = 270.9 Hz), 138.70 (t, J = 2.5 Hz), 110.95, 107.07 (t, J = 24.1 Hz), 100.15 (dd, J_1 = 7.3 Hz, J_2 = 13.4 Hz). FAB MS: 164.0 ([M + H]$^+$).

4,6-Difluoroisophthalaldehyde (14). Compound **13** (410 mg, 2.5 mmol) was dissolved in 10 mL of anhydrous toluene and cooled to 0 °C. DIBAL-H (5 mL of 1.5 M solution in toluene, 7.5 mmol) was added dropwise. The solution was stirred for 1 h at 0 °C. A 15 mL portion of chloroform was then added followed by 25 mL of 10% HCl, and the solution was stirred at room temperature for 1 h. The organic layer was separated followed by extraction with additional 2 × 25 mL of $CHCl_3$. The combined organic layers were washed with 2 × 25 mL of water and dried over anhydrous $MgSO_4$. Purification by silica chromatography (hexanes/CH_2Cl_2, 1:1) gave 285 mg (67%) of **14**. ^{1}H NMR (δ ppm, 500 MHz, $CDCl_3$): 10.29 (s, 2H), 8.46 (t, J = 8.0 Hz, 1H), 7.09 (t, J = 9.8 Hz, 1H). ^{13}C NMR (δ ppm, 125 MHz, $CDCl_3$): 184.63 (t, J = 2 Hz),167.85 (dd, J_1 = 14.6 Hz, J_2 = 269.8 Hz), 131.42 (t, J = 4.8 Hz), 121.74 (dd, J_1 = 4.5 Hz, J_2 = 7.9 Hz), 106.01 (t, J = 24.4 Hz). FAB MS: 170.0 ([M + H]$^+$).

Protected 4,6-Diaminooxyisophthalaldehyde (15). To a solution of **14** (289 mg, 1.7 mmol) and *endo*-*N*-hydroxy-5-norbornene-2,3-dicarboximide (942 mg, 5.1 mmol) in anhydrous DMF (5 mL) was added anhydrous potassium carbonate (705 mg, 5.1 mmol). After the solution was stirred for 1 h, the residue was partitioned between saturated aqueous NaCl (30 mL) and CH_2Cl_2 (30 mL). The water layer was extracted with CH_2Cl_2 (2 × 20 mL). Combined organic layers were washed with brine (4 × 30 mL) and water (2 × 50 mL) and dried over anhydrous $MgSO_4$. After removal of the solvent in vacuo, purification by silica chromatography (10% EtOAc in CH_2Cl_2) yielded 806 mg (97%) of **15**. ^{1}H NMR (δ ppm, 500 MHz, DMSO-d_6): 10.25 (s, 2H), 8.29 (s, 1H), 6.67 (s, 1H), 6.24 (t, J = 2.0 Hz, 4H), 3.59 (m, 4H), 3.39(s, 4H), 1.63 (dd, J_1 = 9 Hz, J_2 = 28 Hz, 4H). ^{13}C NMR (δ ppm, 125 MHz, DMSO-d_6): 186.16, 171.10, 163.38, 135.04, 131.78, 120.93, 100.94, 51.06, 44.37, 42.87. FAB MS: 489.3 ([M + H]$^+$).

Protected 4,6-Diaminooxyisophthalyl Alcohol (16). To a solution of **15** (489 mg, 1.0 mmol) in $CHCl_3$ (48 mL) was added titanium(IV) isopropoxide (0.767 mL, 2.5 mmoL), and the mixture was refluxed for 30 min. After the mixture was cooled to room temperature, methanol (16 mL) and $NaBH_3$-CN (165 mg, 2.5 mmol, in two portions, within 1 h) were added. The residue was partitioned between 100 mL of CH_2Cl_2 and 50 mL of brine and stirred for 1 h. The aqueous layer was extracted twice more with CH_2Cl_2, and the combined organic layers were washed with brine and water, and dried over anhydrous $MgSO_4$. Removal of the solvent followed by silica chromatography (step gradient from 10% EtOAc in CH_2Cl_2 to 50% EtOAc in CH_2Cl_2) resulted in 222 mg (45%) of **16**. ^{1}H NMR (δ ppm, 500 MHz, $CDCl_3$): 7.41 (s, 1H), 6.64 (s, 1H), 6.25 (t, J = 2.0 Hz, 4H), 4.69 (s, 4H), 3.75 (br s, 2H), 3.45 (br s, 4H), 3.31(m, 4H), 1.80 (dt, J_1 = 1.8 Hz, J_2 = 12.5 Hz, 2H), 1.54 (d, J = 9.0 Hz, 2H). ^{13}C NMR (δ ppm, 125 MHz, $CDCl_3$): 172.06, 156.19, 134.84, 131.72, 128.80, 106.77, 59.30, 51.46, 44.85, 42.77.

Protected 4,6-Diaminooxy-α,α′-dibromo-*m*-xylene (17). To a solution of **16** (123 mg, 0.25 mmol) in 10 mL of CH_2Cl_2−ether (1:1) was added PBr_3 (1 M in CH_2Cl_2, 0.30 mL, 0.3 mmol). After being stirred at room temperature for 3 h, the mixture was partitioned between 25 mL of CH_2Cl_2 and 10 mL of water. The organic layer was washed with water (3 × 20 mL), dried over $MgSO_4$, and purified by silica chromatography (1% EtOAc in CH_2Cl_2). Yield: 116 mg (75%). ^{1}H NMR (δ ppm, 300 MHz, DMSO-d_6): 7.68 (s, 1H), 6.41 (s, 1H), 6.19 (s, 4H), 4.70 (s, 4H), 3.50 (br s, 4H), 3.33 (br s, 4H), 1.59 (dd, J_1 = 8.4 Hz, J_2 = 20.7 Hz, 4H). ^{13}C NMR (δ ppm, 75 MHz, DMSO-d_6): 171.32, 156.29, 134.92, 134.04, 122.92, 102.13, 51.10, 44.22, 42.69, 26.61.

Protected 4,6-Diaminooxy-α,α′-di(benzylmethylamine)-*m*-xylene (18). To a mixture of **6** (155 mg, 0.25 mmol) and K_2CO_3 (86.4 mg, 0.625 mmol) in 5 mL of DMSO was added *N*-methylbenzylamine (0.081 mL, 0.625 mmol). After being stirred at room temperature for 2 h, the mixture was partitioned between 25 mL of CH_2 Cl_2 and 10 mL of brine. The organic layer was separated, and the aqueous layer was extracted with CH_2Cl_2 (2 × 10 mL). The combined organic layers were washed with water (4 × 25 mL) and dried over $MgSO_4$. Evaporation of the solvent resulted in the analytically pure product (162.4 mg, 95%). ^{1}H NMR (δ ppm, 500 MHz, $CDCl_3$): 7.79 (s, 1H), 7.39 (d, J = 7.3 Hz, 4H), 7.30 (d, J = 7.3 Hz, 4H), 7.24 (t, J = 7.3 Hz, 2H), 6.60 (s, 1H), 6.26 (s, 4H), 3.79 (s, 4H), 3.57 (s, 4H), 3.47 (s, 4H), 3.29 (m, J = 4.5 Hz,

(27) Schweitzer, B. A.; Kool, E. T. *J. Org. Chem.* **1994**, *59*, 7238−7242.

4H), 2.21 (s, 6H), 1.81 (d, J = 9.0 Hz, 2H), 1.54 (d, J = 9.0 Hz, 2H). ^{13}C NMR (δ ppm, 125 MHz, $CDCl_3$): 171.34, 155.59, 139.52, 134.87, 132.00, 128.85, 128.10, 126.74, 125.87, 104.33, 61.92, 54.34, 51.37, 44.80, 42.84, 42.20. ESI MS (CH_3CN/water 1/3 v/v) 699.6 ($[M + H]^+$).

Synthesis and analytical data of compounds **19**, **20**, **22**, **23**, **25**, **26**, and **28** are described in the Supporting Information.

4-(Protected 2,4-^{15}N-diaminooxybenzyloxy)-*N*,*N* dimethylbenzylamine. To a solution of aldehyde **26** (237.2 mg, 0.42 mmol) in anhydrous $CHCl_3$ (10 mL) was added titanium(IV) isopropoxide (0.84 mmol, 0.250 mL). Dimethylamine hydrochloride (51.4 mg, 0.63 mmol) was then added, and the mixture was refluxed for 30 min. After the mixture was cooled to room temperature, methanol (3.3 mL) and $NaBH_3CN$ (79.2 mg, 1.26 mmol, in two portions, within 1 h) were added. The residue was partitioned between 50 mL of CH_2Cl_2 and 25 mL of brine and stirred for 1 h. The aqueous layer was extracted twice more with CH_2Cl_2, and the combined organic layers were washed with brine and water and dried over anhydrous $MgSO_4$. Removal of the solvent followed by silica chromatography (step gradient from 1 to 8% MeOH in CH_2Cl_2) yielded 130.3 mg (52%) of the product. ^{1}H NMR (δ ppm, 500 MHz, $CDCl_3$): 7.41 (d, J = 9.0 Hz, 1H), 7.29 (d, J = 8.5 Hz, 2H), 7.02 (d, J = 8.5 Hz, 2H), 6.81 (dd, J_1 = 2.5 Hz, J_2 = 8.5 Hz, 1H), 6.76 (d, J = 2.5 Hz, 1H), 6.34 (t, J = 1.8 Hz, 2H), 6.25 (t, J = 1.8 Hz, 2H), 5.26 (s, 2H), 3.79 (s, 2H), 3.51 (dm, J_1 = 3.5 Hz, J_2 = 6.5 Hz, 4H), 3.37 (dm, J_1 = 3.5 Hz, J_2 = 10.5 Hz, 4H), 2.53 (s, 6H), 1.84 (t, J = 9.0 Hz, 2H), 1.58 (t, J = 9.0 Hz, 2H). ^{13}C NMR (δ ppm, 75 MHz, $CDCl_3$): 171.12 (d, J = 9.1 Hz), 171.03, 158.77, 158.19, 155.56, 135.12, 134.93, 131.58, 129.60, 124.27, 121.73, 115.16, 110.62, 102.41, 63.55, 61.67, 51.47, 51.40, 44.79, 44.76, 43.00, 42.90. ESI MS (CH_3CN/water 1/3 v/v) 597.3 ($[M + H]^+$).

Deprotection of Protected Aminooxy Scaffolds. In a typical procedure, varying amount of hydrazine monohydrate was added to a solution of 0.025 mmol of the protected aminooxy scaffold in 1 mL of 10−15% CD_3OD in $CDCl_3$ in an NMR tube, and the deprotection progress was monitored by NMR at room temperature. The pure products were isolated by silica chromatography. Specific conditions used for different scaffolds are given below. ESI MS spectra were recorded in acetonitrile/water 1/3 v/v.

Scaffold 7: 0.063 mmol $H_2NNH_2 \cdot H_2O$, 12 h, solvent evaporated upon completion, silica purification in 2.0% Et_3N in CH_2Cl_2. Yield: 50%. ^{1}H NMR (δ ppm, 400 MHz, DMSO-d_6): 7.59 (s, 1H), 7.22−7.35 (m, 11H), 6.85 (br s, 4H), 3.48 (s, 4H), 3.41 (s, 4H), 2.08 (s, 6H). ESI MS 407.6 ($[M + H]^+$).

Scaffold 8: 0.40 mmol $H_2NNH_2 \cdot H_2O$, 2 h, solvent not evaporated upon completion, silica purification in 1−2% MeOH in CH_2Cl_2. Yield: 55%. ^{1}H NMR (δ ppm, 500 MHz, CD_3CN): 7.21 (d, J = 8.5 Hz, 4H), 7.03 (d, J = 8.5 Hz, 4H), 6.14 (s, 4H), 3.38 (s, 4H), 2.04 (s, 3H). ESI MS 274.5 ($[M + H]^+$).

Scaffold 9: 0.60 mmol $H_2NNH_2 \cdot H_2O$, 3 h, solvent evaporated upon completion, silica purification in 1−3% MeOH in CH_2Cl_2. Yield: 60%. ^{1}H NMR (δ ppm, 400 MHz, DMSO-d_6): 7.26 (dd, J_1 = 8.4 Hz, J_2 = 16.0 Hz, 8H), 6.00 (br s, 4H), 4.51 (s, 4H), 3.44 (s, 4H), 2.03 (s, 3H). ESI MS 302.5 ($[M + H]^+$).

Scaffold 10: 0.10 mmol $H_2NNH_2 \cdot H_2O$, 15 h, solvent evaporated upon completion, silica purification in 2.5% Et_3N in CH_2Cl_2. Yield: 50%. ^{1}H NMR (δ ppm, 500 MHz, DMSO-d_6): 7.26 (d, J = 2.5 Hz, 1H), 7.18 (d, J = 8.5 Hz, 2H), 7.17 (d, J = 8.0 Hz, 1H), 6.96 (s, 2H), 6.95 (s, 1H), 6.91 (d, J = 8.5 Hz, 2H), 6.82 (s, 1H), 6.57 (dd, J_1 = 2.0 Hz, J_2 = 9.0 Hz, 1H), 4.86 (s, 1H), 3.39 (s, 2H), 2.12 (s, 6H). ESI MS 305.2 ($[M + H]^+$).

Scaffold 11: 0.60 mmol $H_2NNH_2 \cdot H_2O$, 2.5 h, solvent not evaporated upon completion, silica purification in 2.5% Et_3N in CH_2Cl_2. Yield: 60%. ^{1}H NMR (δ ppm, 400 MHz, DMSO-d_6): 7.29 (dd, J_1 = 8.8 Hz, J_2 = 14.0 Hz, 4H), 7.21 (d, J = 2.8 Hz,, 1H), 7.14 (d, J = 8.4 Hz, 1H), 6.86 (s, 2H), 6.82 (s, 2H), 6.56 (dd, J_1 = 2.4 Hz, J_2 = 8.4 Hz, 1H), 6.04 (br s, 2H), 4.55 (s, 2H), 3.47 (s, 2H), 3.37 (s, 2H), 2.06 (s, 3H). ESI MS 319.4 ($[M + H]^+$).

Library Formation was performed as described in refs 16 and 17.

Acknowledgment. We are grateful to the NIH for the financial support of this work (Grant No. 6035201 from NIGMS) and Dr. I. Chernushevich (Sciex) for recording the spectrum of compound **5**. The LCMS was obtained with Shared Instrumentation Grant No. S10RR14572 from the National Center for Research Resources, NIH. We thank the Pharmaceutical Sciences instrumentation facility at the University at Buffalo for data acquisition.

Supporting Information Available: Synthesis and analytical data of intermediates, Scheme 2. This material is available free of charge via the Internet at http://pubs.acs.org.

JO015765J